Strong spin–phonon coupling in Gd-filled nanotubes

Venkateswara Rao Sodisetti, Siphephile Ncube, Christopher Coleman, Rudolph M. Erasmus, Emmanuel Flahaut, Somnath Bhattacharyya

Strong spin–phonon coupling in Gd-filled nanotubes

Cite as: J. Appl. Phys. 130, 214301 (2021); doi: 10.1063/5.0067555

V. R. Sodisetti,[1] S. Ncube,[1,2] C. Coleman,[1] R. M. Erasmus,[2] E. Flahaut,[3] and S. Bhattacharyya[1,2,a)]

AFFILIATIONS

[1]Nano Scale Transport Physics Laboratory, School of Physics, University of the Witwatersrand, Johannesburg 2050, South Africa
[2]DSI NRF Centre of Excellence in Strong Materials and School of Physics, University of the Witwatersrand, Johannesburg 2050, South Africa
[3]CIRIMAT, Université de Toulouse, CNRS, INPT, UPS, UMR CNRS UPS INP No. 5085, Université Toulouse Paul Sabatier, Bât. CIRIMAT, 118, route de Narbonne, CEDEX9, Toulouse 31062, France

[a)]**Author to whom correspondence should be addressed:** somnath.bhattacharyya@wits.ac.za

ABSTRACT

To develop one dimensional spintronic devices, we synthesize Gd filled double walled carbon nanotubes where the long spin coherence time of a paramagnetic gadolinium (Gd^{3+}) ion and the discrete phonon modes of a carbon nanotube can be combined. Here, we report Raman observation of spin phonon coupling in the Gd filled double walled nanotubes by analyzing the low temperature dependence of the dominant phonon modes (G band). A G band ($\omega^{+}_{G_{ext}}$ and $\omega^{+}_{G_{int}}$) phonon frequency hardening is observed below a critical temperature of $T_C \sim 110$ K coinciding with the onset temperature of superparamagnetic behavior confirmed through magnetization studies. This anomalous behavior is ascribed to phonon renormalization induced by spin phonon coupling interaction. The estimated spin phonon coupling constant values are 12.2 and 5.0 cm^{-1} for G^{+}_{ext} and G^{+}_{int} phonon modes, respectively, analyzed by comparing the phonon frequency variation ($\Delta\omega$) to magnetization as a function of temperature. Realizing a spin phonon coupling (three times higher than for other multiferroic compounds) interface and modulating it in a one dimensional system have potential benefit when designing effective molecular qubits.

I. INTRODUCTION

Carbon nanotubes (CNTs) have a wide range of applications including single photon emitters,[1] spintronics,[2] and flexible electronics.[3] It is also an encouraging platform for quantum bits owing to its exceptional electron mobility along the π network in one dimensional space. CNT is a diamagnetic material; however, when functionalized with a magnetic material in particular rare earth metal ions, exotic phenomena like Kondo screening of conduction electrons[4] and spin valve[5] features are seen that can be explored for building molecular spintronic devices. The doping concentration of this magnetic molecule on the CNTs can be varied to regulate the magnetic properties of the molecular complex therefore the ability to develop an engineered highly spin correlated system.[6] On the other hand, confinement of various molecules inside the nanotube has also proved to be interesting for exploring fundamental physical and functional properties.[7–9] Thus, one dimensional CNT systems functionalized with magnetic molecules offer an ideal platform for exploring rich atypical physics and exploit specific properties of interest for building electronic applications.

Additionally, carbon nanotube doped with single molecule magnet terbium (III) bis(pthalocyaninato) neutral complex ($TbPc_2$) has already been shown to be an ideal platform for carrying out quantum bit operations.[10,11] The principal operation in this molecular system is based on the spin phonon coupling mechanism where the electron spin of a magnetic ion is coupled to discrete vibrational (phonon) modes of a carbon nanotube relaxing to its equilibrium state through the exchange of quanta of phonon energy.[12] Given the high magnetic anisotropy of 4*f* elements subjected to temperature or an external magnetic field, the resultant magnetization allows magnetic ion spin to change the local CNT lattice vibrational vector direction through phonon emission.[13] Additionally, the spin boson model has recently been widely applied to quantum information processing.[14] Therefore, research

involving the physics of the spin phonon coupled system and the Kondo effect has become particularly important.[4]

Motivated by these interesting findings, we have utilized double walled nanotubes (DWNTs) filled with the rare earth ion Gd^{3+} (having net spin S = 7/2) molecular system to probe spin phonon coupling properties that can potentially be used for carry ing out multi qubit operations. In this communication, we restrict our findings to magnetic studies and spin phonon coupling fea tures observed through low temperature Raman spectroscopy. Optical observation of inelastic scattering events through Raman spectroscopy can be used to study the electronic structures and phonon modes of the nanotubes. Earlier studies were predomi nantly done on DWNTs to differentiate their semiconducting and metallic behavior,[15] observe trends in the phonon frequency change to different filling materials inside the tube,[16] and study the polarization dependence of phonon modes to a polarized angle.[17] However, studies on phonon renormalization concerning spin ordering at low temperatures in a one dimensional material (DWNTs) are scarce. Raman spectroscopy measurements on a single walled carbon nanotube yield two components of the G band: one component is related to the C C bond vibrations along the axis of SWCNT and the other component is related to the C C bond vibrations tangential to the circumference of an SWCNT. The lower wavenumber radial breathing modes (RBMs) are associ ated with radially symmetric expansion and contraction of the SWCNT. The changes in peak position ($\Delta\omega$), peak width ($\Delta\Gamma$), and intensity vary with the temperature. These variations are due to anharmonicity in the vibrational potential and can be explained by the Balkanski model.[18] Particularly for a magnetic material, the phonon mode frequency variation concerning temperature occurs due to anharmonicity ($\Delta\omega_{anh}$) originating from effective lattice interaction in the disordered structure and a spin phonon coupling contribution ($\Delta\omega_{s\ ph}$) coming from the spin ordering of the mag netic ions.[19] Thus, by performing low temperature Raman spectro scopy on the magnetic molecules filled DWNTs, we can analyze the individual contributions and can therefore determine the spin phonon coupling constant through Heisenberg's exchange spin spin correlation function $\langle S_i.S_j \rangle$ in conjugation with magneti zation studies.

II. EXPERIMENTAL METHODS

The DWNT synthesis and their filling were previously reported by us.[20] The Gd filled DWNTs were aligned by DEP using an alternating current of 1 MHz and ±5 V_{pp} voltage. Low temperature magnetic measurements were carried out using a Quantum Design MPMS SQUID magnetometer between the tem peratures 5 and 300 K at an applied field of 100 Oe. Low temperature Raman Spectra were acquired using a 100 × Long Working Distance (LWD) objective (N.A. = 0.80) and a Linkam THMS600 microscope stage and liquid nitrogen as the cryogenic fluid (details are given in the supplementary material).

III. RESULTS AND DISCUSSION

Figures 1(a) and 1(b) show high resolution transmission elec tron microscopy (HRTEM) images of Gd filled DWNTs. Gd nano particles of different shapes (spherical and rod like) are distributed randomly inside the inner tube. Gd is a lanthanide 4*f* series element and shows paramagnetic behavior at room temperature. Furthermore, Gd has a high spin magnetic moment due to its largest possible total spin of S = 7/2.[21] Carbon nanotubes have intrinsic diamagnetism, and their magnetic properties are directly related to π electrons in the graphite lattice. Upon filling the tube with a magnetic material such as the Gd^{3+} ion, the interaction between the Gd spins and with the π network of the inner tube display a collective paramagnetic behavior. Figure 1(c) shows an illustration of Gd ion spins inside a nanotube and their interaction following Heisenberg spin spin correlation function. The temperature dependent magnetization of Gd filled DWNTs is shown in Fig. 1(d), where the magnetic susceptibility $\chi(T)$ was measured between temperatures 5 and 300 K with ZFC and FC.

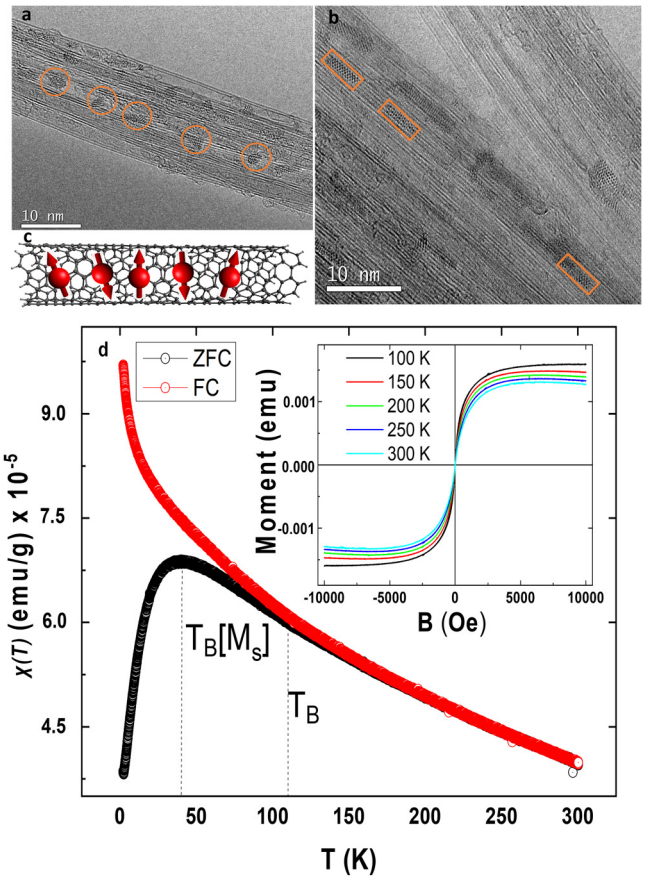

FIG. 1. (a) and (b) HRTEM image of Gd filled DWNTs showing different shapes of Gd ions trapped inside the nanotube. (c) Illustration of the Gd filled DWNT molecular system. (d) SQUID measurements of Gd DWNTs concerning temper ature conducted with ZFC and FC at an applied field of 0.01 T. The difference in the rate of magnetization between FC (red curve) and ZFC (black curve) arises at a critical temperature of T_C (~110 K) and reaches a magnetization saturation at 45 K for ZFC. Inset figure (d): M(H) curves show the superparamagnetic behavior of Gd filled DWNTs.

The magnetic moment of Gd DWNTs shows a bifurcation between FC and ZFC at 110 (±6) K(T_B), indicating the onset of superpara magnetic behavior, and reaches saturation at 45 (±4) K (blocking temperature T_B [M_S]), indicating a dominant superparamagnetic phase.[22] The inset [Fig. 1(d)] shows the same where Gd filled DWNTs showed a superparamagnetic behavior when the magneti zation is swept between positive and negative fields at various temperatures.

Raman spectra were acquired on both pristine and Gd filled DWNTs at different temperatures (80 300 K) using a green laser (E_{laser} = 2.41 eV). The first order Raman spectra of DWNTs consist of low frequency radial breathing modes from ~100 to 300 cm^{-1} [Fig. 2(a)] coming from radially symmetric vibrations and high frequency tangential G band modes from ~1500 to 1650 cm^{-1} [Fig. 2(b)] coming from C C bond vibrations along and tangential to the axis of the inner and outer nanotubes.

RBMs arise due to the cylindrical shape of the nanotube, and in our sample, DWNTs with Lorentzian peaks corresponding to outer (~121 190 cm^{-1}) and inner diameters (~243 270 cm^{-1}) were observed [Fig. 2(a)]. Since we are looking at bundles, we see a range of DWNTs with different diameter distributions, and there will be four different possible configurations of inner and outer nanotube, which are S@S, S@M, M@M, and M@S. By comparing the literature[15] and information from the theoretical Kataura plot[23] with our experimental results, our DWNTs are of M@S configura tion where the inner tube is metallic (E_{11}^{M} transition) and the outer tube (E_{33}^{S} transition) is semiconducting in nature when E = 2.41 eV excitation laser is used. Furthermore, we have used the relation 1 to calculate the RBM frequency of inner and outer tubes, respectively,[24]

$$\omega_{RBM} = \frac{227}{dt}\sqrt{1 + C_{env} d_t^2}, \quad (1)$$

where d_t is diameter of the nanotube and C_{env} accounts for the environmental effect on the RBM frequency; $C_{env} = 0.056\ nm^{-2}$ is considered here. The environmental effects on RBM frequency include intra tube interactions such as alcoholic or functionalized environment and inter tube interactions such as mechanical cou pling between inner and outer tube layers.[25] The diameter of the inner tube d_{in} ranges from 0.84 to 0.93 nm and d_{out} ranges from 1.30 to 1.87 nm for the outer tube and are in good agreement with earlier reports.[26]

It is well established that the electronic property of a nanotube is chiral angle (θ) specific and as well depends on the nanotube diameter.[24] Chiral angle in simple terms is the degree of twisting of the nanotube, which in turn is governed by a chiral vector defined by two integers (n, m).[27] Therefore, when developing an engineer ing application from carbon nanotubes, it is essential to have well defined electronic properties. Since the RBM vibrational signature is unique to carbon nanotubes, its relative intensity can be used to understand the doping effects.[24] From Fig. 2(c), the Lorentzian peaks at ~177 and ~243 cm^{-1} that are associated with the outer diameter and inner diameter of DWNTs, respectively, are down shifted to ~170 and ~241 cm^{-1}, respectively, due to strain induced by filled Gd^{3+} ions. A significant change in intensity is observed in the higher frequency region of RBM related to inner diameter where the intensity of ~241, 255, and ~269 cm^{-1} phonon modes show a steep increase below the critical temperature of $T_c \sim 110$ K [Figs. 2(e) and 2(f)]. This behavior can be ascribed to Gd^{3+} ion spin ordering through exchange interaction (paramagnetic behav ior), changing the local vibronic potential and therefore inducing a strain on both the inner and outer tubes. Further supporting this, their respective intensities as a function of temperature were plotted [Figs. 2(e) and 2(f)]. Corresponding to the onset superpara magnetic phase at ~110 K, the intensities of both modes (~241 and 255 cm^{-1}) showed a significant increase and reaching a maximum at ~90 K.

Now we discuss on G band and how it can be used to charac terize the local C C bonds and in specific how the doping with impurities would influence the C C bond lengths in a nanotube through Raman spectra measurements. For a semiconducting SWNT, five Lorentzian components were reported earlier.[28,29] While for a metallic SWNT, a Lorentzian component and a Breit Wigner Fano (BWF) line shape components were reported.[28] Hence, it can be concluded that the position (ω) and line shape (Γ) of the G band components are different for metallic and semicon ducting CNTs, and therefore, a mix of these G band components would be seen in a M@S configured DWNT.

In Fig. 2(b), the G band of pristine DWNT is deconvoluted into five Lorentzian peaks, with frequencies 1554, 1569, 1576, 1589, and 1596 cm^{-1}. The lower frequency peak of the G band at 1554 cm^{-1} ($\omega_{G_{int}}^{-}$) is assigned as asymmetric BWF line shape of inner metallic nanotube (E_{11}^{M} transition). The BWF line shape can further be expressed by

$$I(\omega) = I_o \frac{\left[1 + \frac{\omega \quad \omega_o}{q\Gamma}\right]^2}{\left[1 + \frac{\omega \quad \omega_o}{\Gamma}\right]^2}, \quad (2)$$

where ω_o and Γ are peak position and FWHM at maximum inten sity I_o, respectively. The $1/q$ value directly correlates to the elec tron phonon coupling strength, and when $1/q$ approaches a zero value, the BWF line shape becomes a Lorentzian function meaning the tube displays semiconducting nature. When $1/q$ reaches unity or greater than 1, the tube displays metallic nature.[30] The peaks at 1589 and 1576 cm^{-1} are associated with $\omega_{G_{ext}}^{+}$(S) mode (LO) and $\omega_{G_{int}}^{+}$(M) mode (TO) corresponding to the C C bond stretching parallel and perpendicular to the nanotube axis, respectively. The peak at 1569 cm^{-1} is assigned as $\omega_{G_{ext}}^{-}$(S) mode. The assignment of LO and TO phonon modes for G^+ band of an outer (S) and inner nanotubes (M), respectively, was considered due to electron phonon coupling (also known as the Kohn anomaly effect) soften ing the LO mode in the case of a metallic nanotube. It becomes more difficult to assign respective modes for both outer semicon ducting and inner metallic nanotubes of a DWNT since both are in resonance with same excitation laser, E = 2.41 eV. The G^+ fre quency values of the outer nanotube (S) at room temperature are closer to the values reported earlier,[31,32] and hence, our evaluation is consistent.

Post filling of Gd^{3+} ion inside DWNT [Fig. 2(d)] we can see from the deconvoluted Raman spectra, only the $\omega_{G_{ext}}^{+}$ and $\omega_{G_{int}}^{+}$

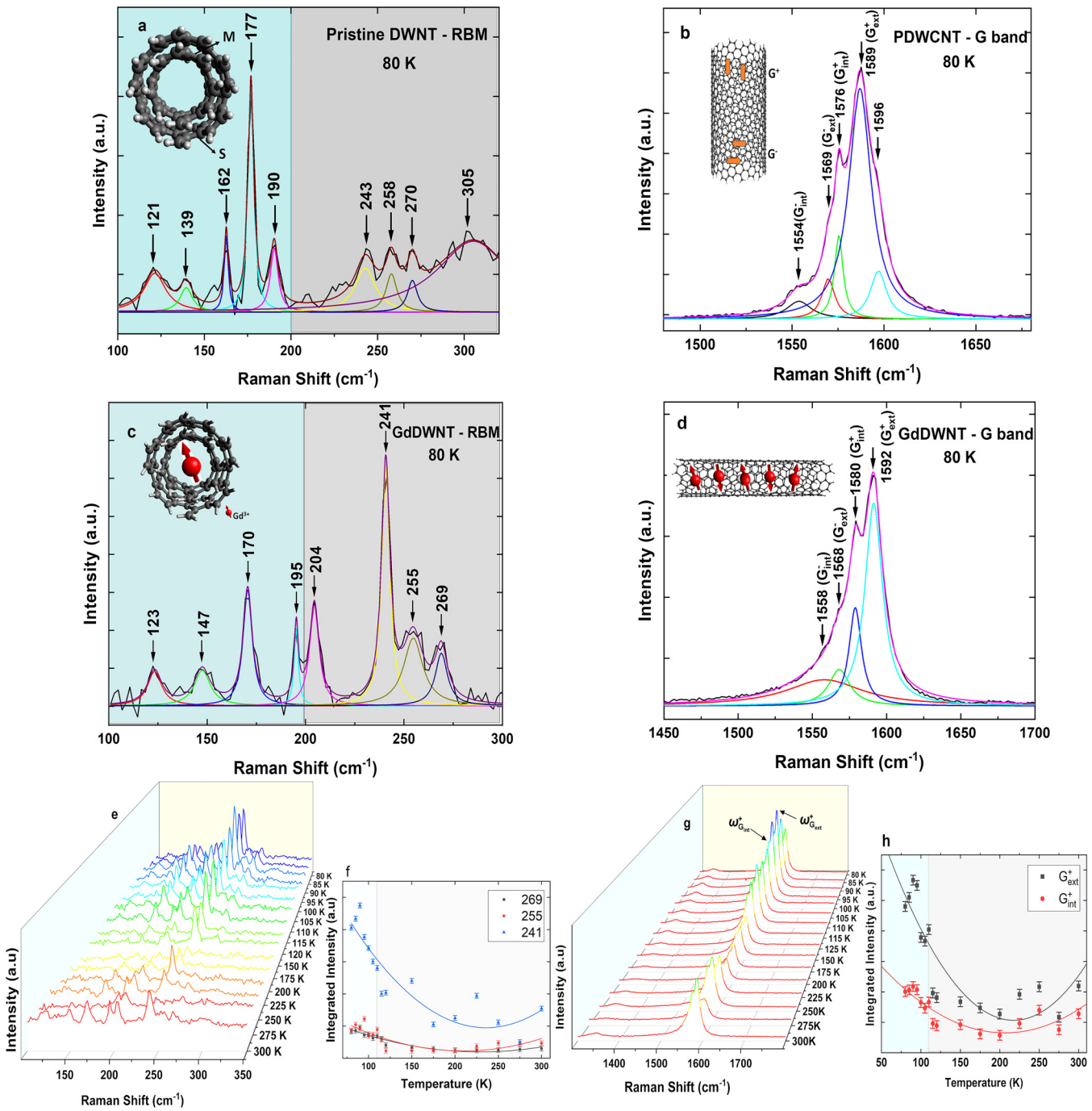

FIG. 2. Raman spectra measured using 514.5 nm excitation wavelength showing both RBM and G band of Pristine and Gd filled DWNTs as a function of temperature. (a) RBMs from 100 to 300 cm^{-1} wavenumber with the blue highlighted region corresponding to the outer tube (Lorentzian peak from ~121 to 190 cm^{-1}) and the gray high lighted region corresponding to the inner tube (Lorentzian peak from ~243 to 270 cm^{-1}) are shown. (b) G band from 1450 to 1650 cm^{-1} is deconvoluted into five different peaks originating from four symmetry modes and one asymmetric (BWF) mode of DWNT. (c) RBM mode of Gd filled DWNTs showing additional peaks associated with filled impurities along with the inner and outer diameter of the tube. (d) Changes in the G band induced by Gd^{3+} ion filling. (e) (h) Integrated intensities plot of RBM and G bands of Gd filled DWNTs as a function of temperature showing a steep increase in their respective intensities below $T_c \sim 110$ K.

symmetry modes associated with the G band are upshifted, while the others such as $\omega^{-}_{G_{ext}}$ mode ($\sim$1568 cm^{-1}) remained same, $\omega^{-}_{G_{int}}$ (BWF line shape $\sim$1554 cm^{-1}) got broader, and highest tangential mode $\sim$1596 cm^{-1} got completely disappeared. This is due to the magnetic Gd^{3+} ion selective screening of conduction electrons in the π network of the nanotube and thereby changing the local deformation potential. As discussed in the Introduction, with decreasing temperature, the G band ($\omega^{+}_{G_{ext}}$ and $\omega^{+}_{G_{int}}$) peak positions are upshifted [Fig. 2(d)], their intensities increased [Figs. 2(g) and 2(h)], and peak widths are reduced ($\Delta\Gamma$) [Fig. S1 in the supplementary material]. The significant observation in the Gd filled DWNTs is frequency shift of both $\omega^{+}_{G_{ext}}$ and $\omega^{+}_{G_{int}}$ positions to higher wave numbers. Furthermore, their respective integrated intensities showed a steep increase below $T_c \sim 110$ K, which indicates that Gd spin changing its local magnetic moment (spin spin exchange interaction) and influencing the π network electrons of both the inner and outer tubes and therefore changing the local vibronic potential, which are in strong resonance with the excited laser, $E = 2.41$ eV [Figs. 2(g) and 2(h)]. In our work, we have used peak position variation for explaining the spin phonon coupling interaction as the uncertainties are less compared with peak width.

In Raman spectra, the phonon mode frequency shift to a lower or higher wavenumber observed at low temperatures arises due to several contributing factors: a pure thermal effect (lattice expansion/contraction), lattice anharmonicity, electro phonon coupling, and spin phonon coupling interaction,

$$\omega(T) = \omega_0 + \Delta\omega_{latt}(T) + \Delta\omega_{anh}(T) + \Delta\omega_{e\ ph}(T) + \Delta\omega_{s\ ph}(T), \quad (3)$$

where ω_0 is the frequency of the phonon at $T = 0$, ω_{latt} is the phonon frequency due to the lattice expansion/contraction, ω_{anh} is the intrinsic anharmonic contribution due to effective lattice interactions, $\omega_{e\ ph}$ is the phonon frequency due to electron phonon coupling, and $\omega_{s\ ph}$ is the spin phonon coupling due to modulation of the exchange integral by lattice vibrations. The tube thermal lattice expansion coefficient and lattice constant values of an SWNT were found to be very small,[33] and hence, the contribution of ω_{latt} to the phonon frequency value at low temperatures is very minimal.

Generally, electron phonon ($\omega_{e\ ph}$) coupling is strong in metallic nanotubes because of the Kohn anomaly effect softening the LO mode. This coupling factor is strongly sample dependent meaning the deformational potential due to local area variations is low or negligible for lowest LO mode when the electrons and phonons are confined to the same region of CNT. It is maximal (>1) when the electronic wavefunction is sharply localized around a region of maximum strain such as doped DWNT where the filled metal impurities would induce a strain on the inner tube. It can also be said that concentration of metal impurities plays a crucial role in determining $\omega_{e\ ph}$ and therefore its influence on the Raman frequency shift. Further literature suggests that this $\omega_{e\ ph}$ is stronger at room temperature due to higher order ground state to excited state vibronic transitions.[34,35] This may not be the case at low temperatures due to low thermal energy for vibronic transitions. Therefore, it is assumed that $\omega_{e\ ph}$ coupling becomes low or negligible at low temperatures. Hence, these two terms (ω_{latt} and $\omega_{e\ ph}$) are neglected during further analysis. Additionally, charge transfer between the shells of nanotube due to functionalization might also induce a frequency shift of the G band;[36,37] however, its influence on the G band frequency shift as a function of temperature is minimal.[38] In particular, the changes in a phonon mode frequency of a magnetic compound as a function of temperature can be attributed due to intrinsic anharmonicity (ω_{anh}) and spin phonon coupling ($\omega_{s\ ph}$) because of magnetic spin ordering at critical temperature. This behavior has already been reported in various magnetic compounds such as $GaFeO_3$,[19] $SrRuO_3$,[39] $BaFe_{12}O_{19}$,[40] $Al_{0.5}Ga_{0.5}FeO_3$,[41] etc.

The anharmonic contribution to the phonon frequency for the first order Raman spectrum of a one dimensional carbon nanotube is due to cubic anharmonicity given by the following equation:[18]

$$\Delta\omega_{anh}(T) = \omega_0 + C\left[1 + \frac{2}{e^x - 1}\right], \quad (4)$$

where $x = \hbar\omega_0/2k_BT$, $\hbar$ is Planck's constant, k_B is Boltzmann constant, and C is an anharmonic constant. This model describes the three photon decay process due to potential anharmonicity in the structure. We neglect the four phonon process as these make a significant contribution only well above room temperature. Figures 3(a) 3(d) show the variation of phonon frequencies of $\omega^{+}_{G_{ext}}$ and $\omega^{+}_{G_{int}}$ modes as a function of temperature for both pristine and Gd filled DWNTs. A nonlinear fit using Eq. (5) to account for the cubic anharmonicity contribution for both the phonon frequency modes of pristine and Gd filled DWNT samples shown as a solid line in Fig. 3. The good fit between the data and the solid curve over most of the temperature range indicates that cubic anharmonicity is a good description of the variation of phonon frequency and that omitting contributions from other processes is justified. At lower temperatures, the slope decreases indicated a weaker contribution from phonon decay processes.[42] However, in our Gd filled DWNT sample, both the $\omega^{+}_{G_{ext}}$ and $\omega^{+}_{G_{int}}$ phonon modes show a clear deviation of the data from the values expected due to anharmonic contribution alone at low temperatures [Figs. 3(b) and 3(d)]. This observation shows a significant phonon hardening by introducing Gd ion inside the DWNT. This is attributed to spin ordering taking place at T_C (110 K) as is shown in magnetization measurements [Fig. 1(d)]. This anomalous hardening due to the spin phonon interaction $\Delta\omega_{s\ ph}(T)$ can be quantified, and this is discussed below.

The deviation in the phonon mode frequency below T_C, i.e, the phonon hardening described above, is due to the spin phonon coupling effect and can be described by

$$\Delta\omega = \omega \quad \omega_0 = \lambda_{s\ ph} \times \langle S_i.S_j \rangle, \quad (5)$$

where ω is the renormalized phonon frequency due to spin phonon interaction at finite low temperature and ω_0 is the phonon frequency in the absence of this interaction. $\lambda_{s\ ph}$ is the spin phonon coupling strength and $\langle S_i.S_j \rangle$ is a spin spin correlation function. The spin spin correlation function can be approximated

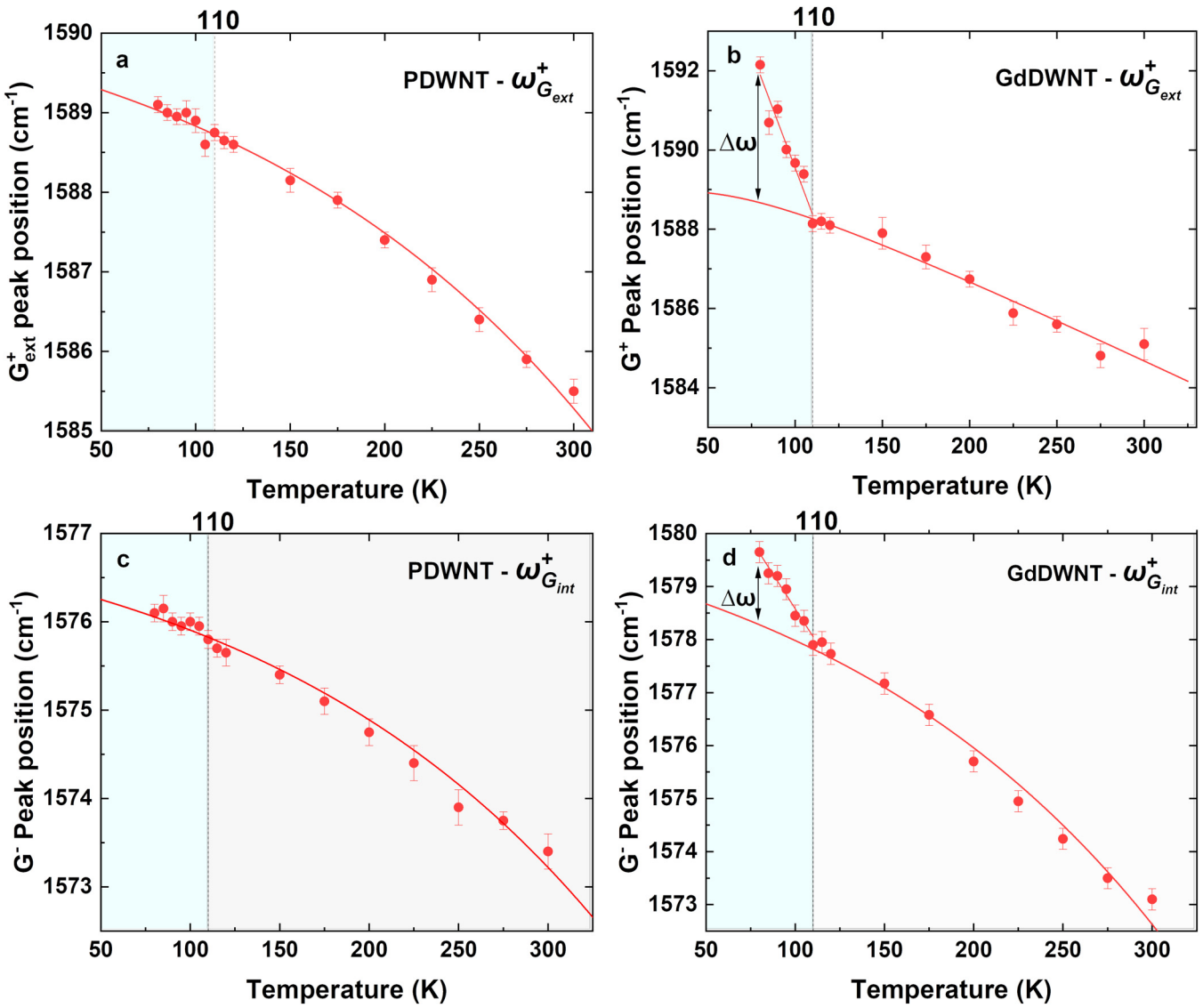

FIG. 3. Variation in phonon mode frequency as a function of temperature. Nonlinear fitting is done using cubic anharmonicity [Eq. (4)]. (a) and (c) phonon mode frequency variation concerning the temperature of $\omega^{+}_{G_{ext}}$ and $\omega^{+}_{G_{int}}$ modes of the pristine DWNTs' sample following a cubic anharmonic decay. (b) and (d) $\omega^{+}_{G_{ext}}$ and $\omega^{+}_{G_{int}}$ modes of Gd filled DWNTs show a deviation in their phonon frequency at a critical temperature of 110 K.

by using the molecular field approximation and $\langle S_i.S_j \rangle$ can be obtained from the ensemble average of nearest neighbor spins,

$$\langle S_i.S_j \rangle = 2\left[\frac{M(T)}{Ms}\right]^2, \tag{6}$$

where $M(T)$ is the magnetization per Gd site magnetic ion and M_S is saturation magnetization. The spin correlations develop as the temperature is decreased, and hence, the spin phonon coupling strength becomes significant when the behavior starts showing superparamagnetic behavior below T_C (~110 K).

The spin phonon coupling strength is found to be larger for the $\omega^{+}_{G_{ext}}$ mode; this can be attributed to the Gd^{3+} electron spin coupled directly with the phonon mode of the DWNT (Fig. 4). A larger λ value also implies this mode is more sensitive to magnetic interaction. The magnetic interaction of Gd^{3+} spin with the $\omega^{+}_{G_{int}}$ mode is weaker for the tangential DWNT phonon mode compared to $\omega^{+}_{G_{ext}}$, yet significant when compared to multiferroic compounds reported earlier.[19,39,40] It is interesting to note that the spin phonon coupling values are approximately *three times higher* than

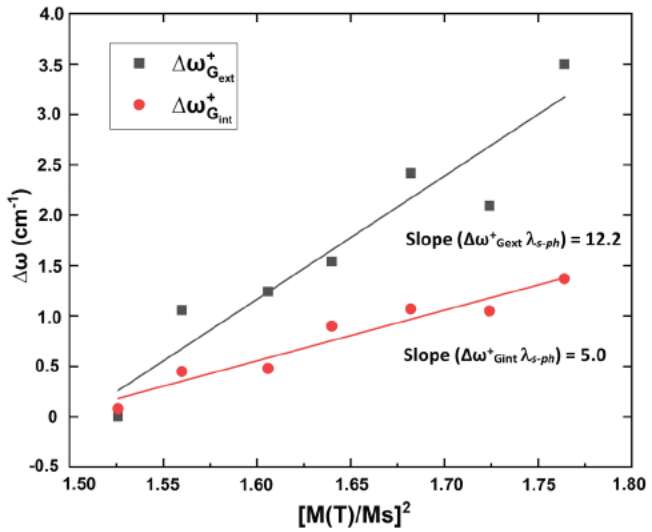

FIG. 4. Plots of the spin phonon frequency component ($\Delta\omega_{s\ ph}$) vs magnetization $\left[\frac{M(T)}{Ms}\right]^2$ are shown for $\omega^+_{G_{ext}}$ and $\omega^+_{G_{int}}$ phonon modes. A linear least square fitting procedure was used to find the spin phonon coupling strength (λ_{s-ph}) (slope of this line).

those of the referenced magnetic compounds. This optical observation of spin phonon coupling strength in a magnetic molecule filled one dimensional system is interesting, and further studies of this system have implications in developing reliable spin qubits through a controlled spin phonon coupling interface between a magnetic ion and DWNT.

The microscopic origin of spin phonon coupling has been studied for nearly 90 years since the original suggestion by Waller and Van Vleck showing how spin dipolar interactions could affect spin relaxation pathways.[43,44] Although the Gd CNT system appears to be more complicated than some molecular systems, a remarkable similarity between these materials has been observed considering CNTs as a 1D molecule having a very distinct Raman feature [Fig. 2(d)]. Modulation of a d electrons' crystal field can be applied to f electron systems. Modulation of an electric field (Stark effect) arises from spin spin interactions, which can produce random magnetic fields that work similarly to the celebrated spin orbit interactions. This leads to phonon renormalization where spin relaxes by coupling to discrete phonon modes in DWNTs as observed in our low temperature Raman data. This can also be verified from the angle dependence of Raman intensity (Fig. 5) where the intensities of both $\omega^+_{G_{ext}}$ and $\omega^+_{G_{int}}$ phonon modes showed a significant increase for Gd filled DWNTs.

It is further shown that the G mode exhibited maximum intensity at $\sim\theta = 0^o$ and minimum at $\sim\theta = 60^o$ due to the relaxation of depolarization effects.[45] The spin phonon mechanism has been interpreted as a three level system by associating one level with the spin flip process, which can be explained in general by the Kondo resonance state. Below the Kondo temperature spin flip from the impurity atoms takes place which can be reflected both from the increase in the resistivity of a sample and from the shift of the Raman frequency.[4] Considering Gd atoms connected to the CNTs as quantum dots, the Gd CNT system can be described as a

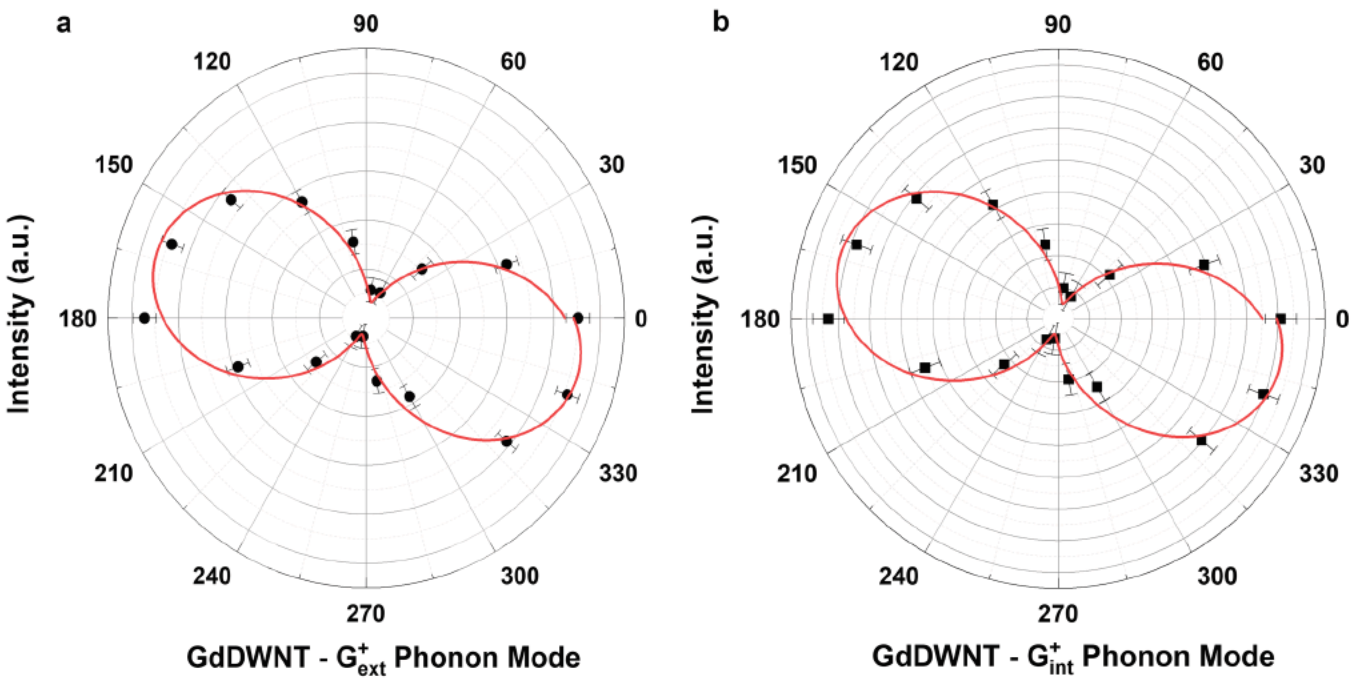

FIG. 5. (a) and (b) Angle dependent Raman intensity for Gd filled DWNTs of $\omega^+_{G_{ext}}$ and $\omega^+_{G_{int}}$ phonon follows sin θ function.

Kondo lattice. This will be discussed in detail in a future publication.

IV. CONCLUSIONS

One dimensional CNTs filled with a magnetic molecule are shown to be a promising platform for developing molecular spin qubits. A rare earth metal filled DWNT based spin system offers an advantage over those based on SWNT. We have experimentally investigated the temperature dependent Raman spectra for magnetic molecule (Gd^{3+}) filled DWNTs and demonstrated the phonon hardening coincides with the onset of superparamagnetic behavior at T_C (110 K). We associate this anomalous phonon hardening behavior of both $\omega^{+}_{G_{ext}}$ and $\omega^{+}_{G_{int}}$ phonon frequencies with the spin phonon coupling interaction due to Gd^{3+} ions inside the DWNTs. It is further shown that the λ_{s-ph} strength in a one dimensional DWNT molecular system is approximately *three times higher* than for other multiferroic compounds reported. This further elucidates the plausibility of engineering a spin qubit network through a 1D DWNT phonon waveguide where Gd^{3+} spins carrying quantum bit information can be coupled with the discrete phonon modes for developing an efficient quantum computation platform.

SUPPLEMENTARY MATERIAL

See the supplementary material for the methodology and plots of peak width (FWHM) variation as a function of temperature.

ACKNOWLEDGMENTS

The authors acknowledge the funding support from the National Research Foundation South Africa under the RSA India bilateral program and BRICS multilateral program. S.B. acknowledges CSIR NLC rental pool project for the generous support to this project and DSI NRF CoESM for the support.

AUTHOR DECLARATIONS

Conflicts of Interest

The authors have no conflicts to disclose.

DATA AVAILABILITY

The data that support the findings of this study are available from the corresponding author upon reasonable request.

REFERENCES

[1]A. H. Brozena, M. Kim, L. R. Powell, and Y. H. Wang, Nat. Rev. Chem. **3**, 375 (2019).
[2]F. Kuemmeth, H. O. H. Churchill, P. K. Herring, and C. M. Marcus, Mater. Today **13**, 18 (2010).
[3]L. Xiang, H. Zhang, Y. Hu, and L. M. Peng, J. Mater. Chem. C **6**, 7714 (2018).
[4]S. Ncube, C. Coleman, A. Strydom, E. Flahaut, A. De Sousa, and S. Bhattacharyya, Sci. Rep. **8**, 1 (2018).
[5]M. Urdampilleta, S. Klyatskaya, J. P. Cleuziou, M. Ruben, and W. Wernsdorfer, Nat. Mater. **10**, 502 (2011).
[6]I. S. Mosse, V. R. Sodisetti, C. Coleman, S. Ncube, A. S. de Sousa, R. M. Erasmus, E. Flahaut, T. Blon, B. Lassagne, T. Šamořil, and S. Bhattacharyya, Molecules **26**, 563 (2021).
[7]C. E. Giusca, V. Stolojan, J. Sloan, F. Börrnert, H. Shiozawa, K. Sader, M. H. Rümmeli, B. Büchner, and S. R. P. Silva, Nano Lett. **13**, 4020 (2013).
[8]J. Sloan, A. I. Kirkland, J. L. Hutchison, and M. L. H. Green, Chem. Commun. **2**, 1319 (2002).
[9]J. H. Spencer, J. M. Nesbitt, H. Trewhitt, R. J. Kashtiban, G. Bell, V. G. Ivanov, E. Faulques, J. Sloan, and D. C. Smith, ACS Nano **8**, 9044 (2014).
[10]E. Moreno-Pineda, C. Godfrin, F. Balestro, W. Wernsdorfer, and M. Ruben, Chem. Soc. Rev. **47**, 501 (2018).
[11]M. Ganzhorn, S. Klyatskaya, M. Ruben, and W. Wernsdorfer, Nat. Nanotechnol. **8**, 165 (2013).
[12]A. Lunghi and S. Sanvito, Sci. Adv. **5**, 1 (2019).
[13]E. M. Chudnovsky, D. A. Garanin, and R. Schilling, Phys. Rev. B **72**, 094426 (2005).
[14]P. C. Baral and G. C. Rout, Prog. Theor. Phys. **126**, 1101 (2011).
[15]F. Villalpando-Paez, H. Son, D. Nezich, Y. P. Hsieh, J. Kong, Y. A. Kim, D. Shimamoto, H. Muramatsu, T. Hayashi, M. Endo, M. Terrenes, and M. S. Dresselhaus, Nano Lett. **8**, 3879 (2008).
[16]M. Sendova, E. Flahaut, and T. Hartsfield, J. Appl. Phys. **108**, 044309 (2010).
[17]W. Ren, F. Li, and H. M. Cheng, Phys. Rev. B **71**, 115428 (2005).
[18]M. Balkanski, R. F. Wallis, and E. Haro, Phys. Rev. B **28**, 1928 (1983).
[19]S. Dugu, K. K. Mishra, D. K. Pradhan, S. Kumari, and R. S. Katiyar, J. Appl. Phys. **125**, 064101 (2019).
[20]E. Flahaut, R. Bacsa, A. Peigney, and C. Laurent, Chem. Commun. **3**, 1442 (2003).
[21]J. F. Elliott, S. Legvold, and F. H. Spedding, Phys. Rev. **91**, 28 (1953).
[22]S. Ncube, C. Coleman, E. Flahaut, S. Bhattacharyya, A. R. E. Prinsloo, and C. J. Sheppard, AIP Adv. **11**, 035206 (2021).
[23]G. G. Samsonidze, R. Saito, N. Kobayashi, A. Grüneis, J. Jiang, A. Jorio, S. G. Chou, G. Dresselhaus, and M. S. Dresselhaus, Appl. Phys. Lett. **85**, 5703 (2004).
[24]A. Jorio and R. Saito, J. Appl. Phys. **129**, 021102 (2021).
[25]S. Öberg, J. J. Adjizian, D. Erbahar, J. Rio, B. Humbert, M. Dossot, A. Soldatov, S. Lefrant, J. Y. Mevellec, P. Briddon, M. J. Rayson, and C. P. Ewels, Phys. Rev. B **93**, 045408 (2016).
[26]M. Erkens, S. Cambré, E. Flahaut, F. Fossard, A. Loiseau, and W. Wenseleers, Carbon **185**, 113 (2021).
[27]R. F. Rajter, R. H. French, W. Y. Ching, R. Podgornik, and V. A. Parsegian, RSC Adv. **3**, 823 (2013).
[28]A. Jorio, A. G. Souza Filho, G. Dresselhaus, M. S. Dresselhaus, A. K. Swan, M. S. Ünlü, B. B. Goldberg, M. A. Pimenta, J. H. Hafner, C. M. Lieber, and R. Saito, Phys. Rev. B **65**, 155412 (2002).
[29]M. S. Dresselhaus and P. C. Eklund, Adv. Phys. **49**, 705 (2000).
[30]M. Sendova and E. Flahaut, J. Appl. Phys. **103** 024311 (2008).
[31]J. Marquina, C. H. Power, J. M. Broto, E. Flahaut, and J. Gonzalez, Rev. Mex. Fis. **57**, 510 517 (2011), see http://www.scielo.org.mx/scielo.php?script=sci_abstract&pid=S0035-001X2011000600007&lng=pt&nrm=iso&tlng=en.
[32]J. Arvanitidis, D. Christofilos, K. Papagelis, K. S. Andrikopoulos, T. Takenobu, Y. Iwasa, H. Kataura, S. Ves, and G. A. Kourouklis, Phys. Rev. B **71**, 125404 (2005).
[33]Y. Maniwa, R. Fujiwara, H. Kira, H. Tou, H. Kataura, S. Suzuki, Y. Achiba, E. Nishibori, M. Takata, M. Sakata, A. Fujiwara, and H. Suematsu, Phys. Rev. B **64**, 241402 (2001).
[34]H. Suzuura and T. Ando, Phys. Rev. B **65**, 235412 (2002).
[35]R. Leturcq, C. Stampfer, K. Inderbitzin, L. Durrer, C. Hierold, E. Mariani, M. G. Schultz, F. von Oppen, and K. Ensslin, Nat. Phys. **5**, 327 (2009).
[36]M. Kalbac, A. A. Green, M. C. Hersam, and L. Kavan, Chem. Eur. J. **17**, 9806 (2011).
[37]P. Puech, A. Ghandour, A. Sapelkin, C. Tinguely, E. Flahaut, D. J. Dunstan, and W. Bacsa, Phys. Rev. B **78**, 045413 (2008).
[38]P. Puech, T. Hu, A. Sapelkin, I. Gerber, V. Tishkova, E. Pavlenko, B. Levine, E. Flahaut, and W. Bacsa, Phys. Rev. B **85**, 205412 (2012).
[39]S. G. Jeong, S. Y. Lim, J. Kim, S. Park, H. Cheong, and W. S. Choi, Nanoscale **12**, 013926 (2020).

[40]X. B. Chen, N. T. Minh Hien, K. Han, J. Chul Sur, N. H. Sung, B. K. Cho, and I. S. Yang, J. Appl. Phys. **114**, 013912 (2013).
[41]K. K. Mishra, R. Shukla, P. S. R. Krishna, P. D. Babu, S. N. Achary, R. S. Katiyar, and J. F. Scott, Phys. Chem. Chem. Phys. **22**, 6906 (2020).
[42]P. Verma, S. C. Abbi, and K. P. Jain, Phys. Rev. B **51**, 016660 (1995).
[43]J. J. H. Van Vleck, Phys. Rev. **57**, 426 (1940).
[44]I. Waller, Z. Phys. **79**, 370 (1932).
[45]A. M. Rao, A. Jorio, M. A. Pimenta, M. S. S. Dantas, R. Saito, G. Dresselhaus, and M. S. Dresselhaus, Phys. Rev. Lett. **84**, 1820 (2000).